



Demixing, surface nematization, and competing adsorption in binary mixtures of hard rods and hard spheres under confinement

DOI:

[10.1063/1.5020002](https://doi.org/10.1063/1.5020002)

Document Version

Accepted author manuscript

[Link to publication record in Manchester Research Explorer](#)

Citation for published version (APA):

Wu, L., Malijevsky, A., Avendano, C., Müller, E. A., & Jackson, G. (2018). Demixing, surface nematization, and competing adsorption in binary mixtures of hard rods and hard spheres under confinement. *The Journal of chemical physics*. <https://doi.org/10.1063/1.5020002>

Published in:

The Journal of chemical physics

Citing this paper

Please note that where the full-text provided on Manchester Research Explorer is the Author Accepted Manuscript or Proof version this may differ from the final Published version. If citing, it is advised that you check and use the publisher's definitive version.

General rights

Copyright and moral rights for the publications made accessible in the Research Explorer are retained by the authors and/or other copyright owners and it is a condition of accessing publications that users recognise and abide by the legal requirements associated with these rights.

Takedown policy

If you believe that this document breaches copyright please refer to the University of Manchester's Takedown Procedures [<http://man.ac.uk/04Y6Bo>] or contact uml.scholarlycommunications@manchester.ac.uk providing relevant details, so we can investigate your claim.



1 Demixing, surface nematization, and competing adsorption in binary mixtures 2 of hard rods and hard spheres under confinement

3 Liang Wu,^{1,2} Alexandr Malijevský,^{3,4} Carlos Avendaño,⁵ Erich A. Müller,¹ and George Jackson¹

4 ¹*Department of Chemical Engineering, Imperial College London, South Kensington Campus, London, SW7 2AZ,*
5 *United Kingdom*

6 ²*School of Chemistry and Chemical Engineering, Shanghai Jiao Tong University, Shanghai, China,*
7 *200240*

8 ³*Department of Physical Chemistry, University of Chemical Technology Prague, 166 28 Praha 6,*
9 *Czech Republic*

10 ⁴*Department of Microscopic and Mesoscopic Modelling, ICPF of the Czech Academy of Sciences, 165 02 Prague 6,*
11 *Czech Republic*

12 ⁵*School of Chemical Engineering and Analytical Science, The University of Manchester, Sackville Street,*
13 *Manchester M13 9PL, United Kingdom*

14 (Dated: 20 March 2018)

A molecular simulation study of binary mixtures of hard spherocylinders (HSCs) and hard spheres (HSs) confined between two structureless hard walls is presented. The principal aim of the work is to understand the effect of the presence of hard spheres on the entropically-driven surface nematization of the hard rod-like particles at the walls. The mixtures are studied using a constant normal-pressure Monte Carlo algorithm. The surface adsorption at different compositions of hard spheres is examined in detail. At moderate hard-sphere concentrations preferential adsorption of the spheres at the wall is found. However, at moderate to high pressure (density), we observe a crossover in the adsorption behaviour with nematic layers of the rods forming at the walls leading to a local demixing of the system. The presence of the spherical particles is seen to destabilize the surface nematization of the rods, and the degree of demixing increases on increasing the HS concentration.

15 I. INTRODUCTION

16 Particle shape is one of the most important fea-
17 tures governing the collective behaviour of colloidal
18 suspensions^{1,2}. As the shape of a particles deviates from
19 spherical geometry, a rich phase behaviour emerges due
20 to the additional orientational degrees of freedom giving
21 rise to a variety of complex crystal, plastic crystal, and
22 liquid crystals (LC) structures.³⁻⁷ Colloidal particles are
23 also attractive as model systems to study various physical
24 phenomena due to the possibility of controlling the range,
25 strength, and form of the interparticle interactions, even
26 to the limit of designing interactions that are purely re-
27 pulsive at short range, i.e., approaching the hard-core in-
28 teraction limit⁸. In his pioneering work in 1949, Onsager⁹
29 offered a successful explanation for the isotropic-nematic
30 phase transition observed in uniaxial anisotropic parti-
31 cles such as thin rods modelled as hard spherocylinders
32 (HSCs): cylinders of diameter D and length L capped
33 at each end by hemispheres of diameter D . Onsager de-
34 scribed the isotropic-nematic phase transition as a com-
35 petition between the orientational entropy, which favours
36 the stabilization of isotropic (Iso) phases, and the packing
37 (free-volume) entropy which induces the alignment of the
38 particles thus promoting the formation of nematic (Nem)
39 phases. Onsager's second-virial theory provides a good
40 description of rod-like particles in the limit of extreme
41 shape anisotropies corresponding to $L/D \rightarrow \infty$ in the
42 case of HSCs¹⁰. As the aspect ratio L/D of the particles
43 is decreased, the theory becomes less reliable and more
44 accurate methods such as higher-order density functional
45 theories (DFTs)^{11,12} and computer simulations^{10,13} are

46 required to accurately describe the ordering transitions.

47 The phase behaviour of non-spherical particles be-
48 comes even more complex in the presence of external po-
49 tentials such as electromagnetic fields, gravity, and geo-
50 metric confinement¹⁴. The behaviour of rod-like particles
51 in contact with solid substrates modelled as hard struc-
52 tureless walls have been studied extensively¹⁵⁻¹⁷. The
53 broken spatial symmetry along the normal direction to
54 the wall induces additional phenomena, such as anchor-
55 ing (see Ref.¹⁶ for a review), in which the orientation of
56 the particles at the wall is different to that in the bulk
57 system; in some cases the extent of the surface orientation
58 may be of a macroscopic dimension. The influence of the
59 alignment of the particles at the wall on the isotropic-
60 nematic transition has been studied theoretically us-
61 ing a variety of approaches including phenomenological
62 Landau-de Gennes theory¹⁸, mean-field DFT¹⁹⁻²¹, and
63 generalized Onsager theory²²⁻²⁵. A second-virial On-
64 sager theory has been employed by van Roij *et al.*²⁶ to
65 study confined rectangular rods in which the orientations
66 of the particles are restricted to three possible directions
67 (the Zwanzig model): a continuous uniaxial-biaxial ne-
68 matic surface phase transition was found for an isotropic
69 fluid in contact with a single planar hard wall, followed
70 by wetting of the wall by a nematic film comprised of
71 particles oriented parallel to the wall corresponding to
72 homogeneous (planar) alignment. The appearance of the
73 nematic film was found to occur before the phase tran-
74 sition to a bulk nematic phase away from the wall. A
75 first-order capillary nematization transition was observed
76 when the fluid was confined between two parallel hard
77 walls with a capillary critical point for wall intersepa-

78 rations of about twice the length of the rods. Using a
 79 similar model, Aliabadi *et al.*²⁷ showed that the width of
 80 the nematic film diverges logarithmically as the density
 81 of the systems approaches the isotropic-nematic transi-
 82 tion. The effect of confinement on the positional order
 83 and smectic layering of aligned hard cylinders has also
 84 been studied using the Onsager free-energy functional²⁸.
 85 More recently, the surface induced phase transitions of
 86 semi-flexible polymer chains confined between two par-
 87 allel walls have been studied using a self-consistent field
 88 theory²⁹. Despite these efforts, an accurate theoretical
 89 description of liquid crystalline ordering near solid sur-
 90 faces remains very challenging (see Ref.³⁰ for a recent
 91 review).

92 Computer simulation studies of various non-spherical
 93 particles either under confinement or in the presence of
 94 a solid substrate have been reported for a wide vari-
 95 ety of model systems including hard spherocylinders^{31–36},
 96 hard needles²⁵, hard ellipsoids^{37,38}, hard cut spheres^{35,39},
 97 spherical caps⁴⁰, hard dimers⁴¹, hard Gaussian over-
 98 lap particles⁴², Gay-Berne particles^{43–46}, and board-like
 99 Zwanzig models²⁶, as well as system of spherical particles
 100 decorated with an anisotropic Lennard-Jones potential⁴⁷,
 101 semiflexible polymer chains^{48–51}, and rod-like particles
 102 with chiral interactions^{52,53}. Several types of surface-
 103 particle potentials and heterogeneities including surface
 104 roughness⁵⁴, softness³⁹, surface anchoring¹⁷, competing
 105 walls⁵⁵, and spherical confinement⁵⁶ have also been ex-
 106 amined in simulations of confined liquid crystals. In par-
 107 ticular, the work of Mao *et al.*³² and Dijkstra *et al.*³³
 108 provides an excellent analysis of the adsorption, structure
 109 and orientation of hard spherocylinders at the surface of
 110 the wall. Mao *et al.*³², for example, have reported Monte
 111 Carlo (MC) simulations of hard spherocylinders (with as-
 112 pect ratios of $L/D = 10$ and 20) confined between two
 113 parallel hard structureless walls for states of relatively
 114 low density; the emphasis of their work was understand-
 115 ing the depletion forces induced by the walls, the surface
 116 adsorption, and the quantification of the surface tension
 117 for the isotropic fluid in contact with the wall. In their
 118 thorough simulation study, Dijkstra *et al.*³³ examine the
 119 behaviour of hard spherocylinders in contact with a sin-
 120 gle wall (allowing the thickness of the nematic film to
 121 diverge) investigating the surface adsorption and nema-
 122 tization of hard spherocylinders with an aspect ratio of
 123 $L/D = 15$. Simulation studies of the hard spherocylinders
 124 with $L/D = 10$ confined between two impenetrable
 125 parallel hard walls have been carried out to determine the
 126 profiles of the number density, nematic order parameter,
 127 degree of biaxiality, and normal and tangential compo-
 128 nents of the pressure tensor which allow one to obtain
 129 the fluid-wall interfacial tension of the system deep into
 130 the liquid-crystalline region^{57,58}. Savenko and Dijkstra⁵⁹
 131 also analysed the sedimentation and phase equilibria of
 132 hard spherocylinders on a planar hard wall observing the
 133 formation of nematic, smectic, and even crystal phases.

134 From the experimental perspective, liquid crystalline
 135 phases observed in suspensions of colloidal particles such

136 as vanadium pentoxide (V_2O_5)⁶⁰, Gibbsite ($Al(OH)_3$)
 137 platelets^{61,62}, carbon nanotubes⁶³, and some biologi-
 138 cal systems such as protein fibers⁶⁴, tobacco mosaic
 139 virus⁶⁵, *fd*-virus^{66,67}, polypeptide solutions^{68,69}, and
 140 DNA chains⁷⁰ offer convenient test beds for an assess-
 141 ment of the simple hard core models of mesogenic sys-
 142 tems. The work by Galanis *et al.*⁷¹ provides a very use-
 143 ful insight into the surface behaviour of granular rod-like
 144 particles (with aspect ratios of $L/D \sim 20$) for very thin
 145 layers of rods in a quasi-2D circular container. The num-
 146 ber density profiles measured are in excellent agreement
 147 with previous findings from computer simulations. The
 148 influence of a flat wall on the surface anchoring of col-
 149 loidal rods has been examined for aqueous suspensions
 150 of silica particles⁷². As with other colloidal systems of
 151 this type, the silica rods show a similar behavior to the
 152 athermal (purely repulsive) system and are of sufficiently
 153 low polydispersity to allow the formation of nematic and
 154 and smectic phases with increasing particle concentra-
 155 tion. Good agreement is found with corresponding re-
 156 sults obtained from computer simulations of hard spher-
 157 ocylinders^{10,11,13,73–76}. This interesting work provides
 158 experimental confirmation that rod-like particles adopt a
 159 planar anchoring configuration in the vicinity of the sur-
 160 face. In this experimental analog of the hard-core system,
 161 the effect of the surface spans over tens of microns.

162 Beside the aforementioned studies dealing with one-
 163 component liquid-crystalline systems, there is a large
 164 body of work devoted to modelling and understanding
 165 the phase behaviour of athermal mixtures of mesogenic
 166 components including rod-rod^{67,77–80}, rod-sphere^{81–91},
 167 rod-disc^{92–99} and disc-disc^{100,101} and disc-sphere¹⁰² hard-
 168 core systems. The reader is directed to Reference 103 for
 169 a more detailed discussion. Although theoretical studies
 170 of binary mixtures of rod-like and spherical particles in
 171 the presence of structureless solid substrates have been
 172 reported^{85,104}, computer simulation studies of rod-sphere
 173 mixtures under confinement in the form of a slit pore are
 174 scarce⁹¹.

175 It is the purpose of our current paper to fill this gap.
 176 Here, we study the adsorption behaviour of binary mix-
 177 tures of hard spheres and hard spherocylinders confined
 178 by parallel hard wall using Monte Carlo simulation. This
 179 model system is entirely athermal and hence its proper-
 180 ties are governed by purely entropic effects. In our pre-
 181 vious work⁹¹, we described the isotropic-nematic phase
 182 behaviour of the mixture in bulk. We now extend this
 183 study by assessing the effect of hard walls on formation
 184 of nematic films at conditions where only an isotropic
 185 phase is stable in the bulk. In particular, we examine
 186 the trade off between the stabilization of the nematic
 187 phase by presence of the wall and destabilizing effect of
 188 the hard spheres on the orientational order of the system.

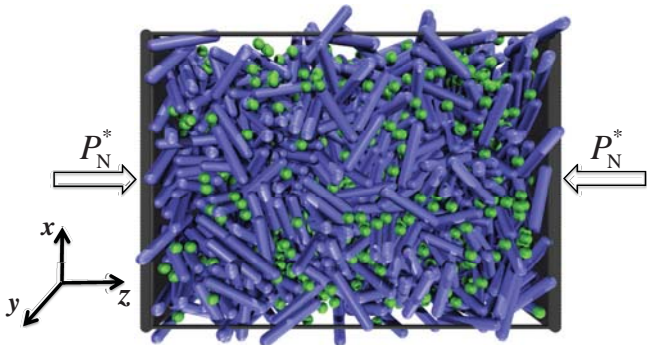


FIG. 1. Geometry and simulation set up used in our $NP_N T$ Monte Carlo simulations to study binary mixtures of hard spherocylinders (blue) and hard spheres (green) confined between two hard walls. The parallel hard walls are placed along the z axis and the equilibrium (normal) pressure P_N is applied perpendicularly to the walls.

189 II. SIMULATION DETAILS

190 The methodology employed in our current work is similar to that described in a previous paper⁹¹. Binary
191 mixtures of hard spherocylinders and hard spheres confined between two hard walls are studied using constant
192 normal-pressure Monte Carlo simulation ($NP_N T$ -MC), where N is the total number of particles, P_N is the normal
193 pressure (directed perpendicular to the wall), and T is the absolute temperature. Strictly speaking, the surface
194 area A and the global composition of the mixture should be included in the designation of the ensemble
195 but we choose to retain the $NP_N T$ abbreviation for conciseness, bearing in mind that the latter variables are
196 also kept constant. Throughout our simulations, the number of hard spherocylinders with an aspect ratio
197 $L/D = 5$ is fixed at $N_{\text{HSC}} = 1482$ while the number of hard spheres N_{HS} , also of a diameter D , is varied to
198 specify the hard-sphere mole fraction (composition) given by $x_{\text{HS}} = N_{\text{HS}}/N$ where $N = N_{\text{HS}} + N_{\text{HSC}}$.
199

200 The geometry of the simulation set up is shown in Figure 1. We consider a rectangular simulation box with
201 standard Cartesian coordinates oriented along the box edges. Two parallel hard structureless walls are positioned
202 at $z = 0$ and $z = L_z$ along the z axis and standard periodic boundary conditions are applied along the x and
203 y directions. The volume of the system is allowed to fluctuate during the $NP_N T$ -MC simulations by varying the
204 dimension of the z axis (L_z), while the dimensions of the system along the x and y axes ($L_x = L_y = 25D$) are kept
205 fixed. For systems with this planar symmetry the condition of mechanical equilibrium ($\nabla \cdot \mathbf{P} = 0$) requires that
206 the normal component of the pressure tensor is constant throughout the sample, and as a consequence the normal
207 component is also equivalent to the equilibrium pressure of the system. With N_{HSC} fixed, we may choose the following
208 thermodynamic parameters to define a given system: the composition x_{HS} , the normal pressure P_N , and

226 the surface area of the x - y plane ($A = L_x L_y = 625D$).

227 The $NP_N T$ -MC simulations are performed for 5×10^6
228 cycles to equilibrate the system and $5 - 8 \times 10^6$ cycles to accumulate ensemble averages. Each MC cycle
229 consists of N attempts to displace (and rotate in case of the hard spherocylinders) a randomly chosen molecule
230 and one trial volume change in which the z dimension is scaled. The breaking of symmetry caused by the hard
231 walls leads to inhomogeneous positional and orientational distributions of the particles along the z axis. In order
232 to evaluate the one-body number density profile $\rho_i(z)$, for $i = \{\text{HS}, \text{HSC}\}$, the composition profile $x_i(z)$, and
233 the nematic order parameter profile $S_2(z)$, the simulation box is divided into n_{bin} bins of equal width δz along the
234 z direction. The density profile $\rho_i(z)$ is calculated as

$$\rho_i(z) = \frac{\langle N_i(z) \rangle D^3}{L_x L_y \delta z} \quad \text{for } i = \text{HS}, \text{HSC}, \quad (1)$$

241 where $\langle N_i(z) \rangle$ represents the ensemble average of the local number of particles of component i at position z .
242 Typically $n_{\text{bin}} = 200$ bins are used for the calculations. The local composition profile $x_i(z)$ of the mixture is de-
243 termined as

$$x_i(z) = \frac{\rho_i(z)}{\rho_{\text{HS}}(z) + \rho_{\text{HSC}}(z)} \quad \text{for } i = \text{HS}, \text{HSC}. \quad (2)$$

246 Provided the system is sufficiently large, one expects that the structural and thermodynamic quantities determined
247 from the central part of the box are consistent with the corresponding bulk limits. In particular, the density profiles
248 $\rho_{\text{HSC}}(z)$ and $\rho_{\text{HS}}(z)$ are expected to reach the values of the corresponding bulk densities of $\rho_{\text{HSC},b}$ and $\rho_{\text{HS},b}$
249 far away from the wall. Having determined the bulk densities, the adsorption Γ_i of each component can be quan-
250 tified from the following integral:

$$\Gamma_i = \frac{1}{D} \int_0^{L_z} [\rho_i(z) - \rho_{i,b}] dz \quad \text{for } i = \text{HS}, \text{HSC} \quad (3)$$

255 It is important to note that in the case of our confined system the overall volume of the system includes the
256 two regions inaccessible to the hard particles in layers of thickness $D/2$ close to the two walls.

259 The orientational order of the hard-spherocylindrical rods is quantified using the average of the second Legendre
260 polynomial S_2 ¹⁰⁵ of relative orientation the principle axis of the particles with respect to the nematic director.
261 The nematic order parameter profile $S_2(z)$ is obtained by determining the Saupe ordering tensor $\mathbf{Q}(j)$ in each bin
262 j :

$$\mathbf{Q}(j) = \left\langle \frac{1}{2N_{\text{HSC},j}} \sum_{i=1}^{N_{\text{HSC},j}} (3\hat{\omega}_i \otimes \hat{\omega}_i - \mathbf{I}) \right\rangle \quad (4)$$

266 where $\hat{\omega}_i$ is the orientation of rod i , $N_{\text{HSC},j}$ is the number of hard spherocylinders in bin j , and \mathbf{I} is the unit tensor.
267 On diagonalization of the $\mathbf{Q}(j)$ tensor¹⁰⁶, three eigenvalues are obtained and the largest value is defined as the

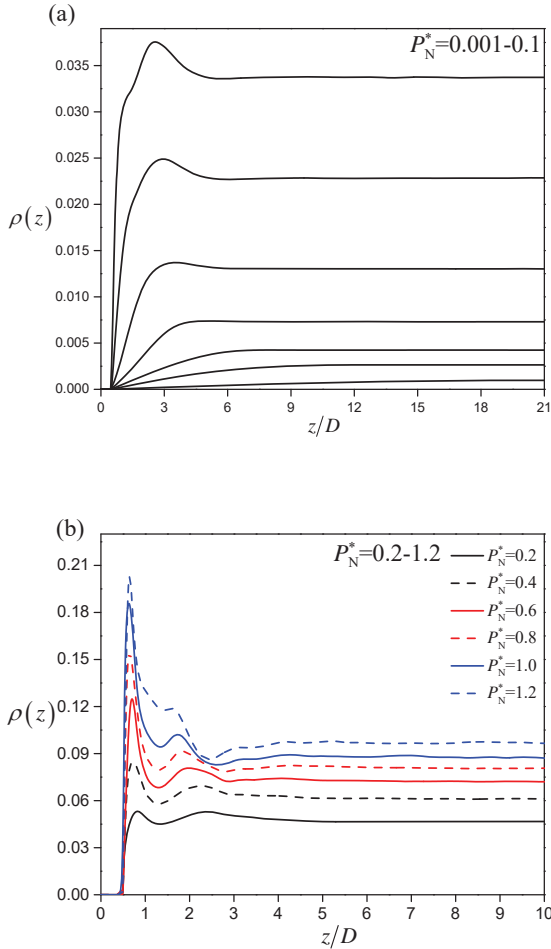


FIG. 2. Density profiles $\rho(z)$ for a system of pure $L/D = 5$ hard spherocylinders confined between parallel hard walls obtained from $NP_N T$ -MC simulation along the normal direction to the wall. The curves correspond to the equilibrium (normal) pressures of (from bottom to top): (a) $P_N^* = [0.001, 0.003, 0.005, 0.01, 0.02, 0.05, 0.1]$; and (b) $P_N^* = [0.2 - 1.2]$ in increments of $\Delta P_N^* = 0.2$.

local nematic order parameter $S_2(z)$ associated with bin j . Some care should be taken with the calculation of the order parameter profile due to finite-size effects. Eppenga and Frenkel¹⁰⁷ have shown that the order parameter depends on the number of mesogenic particles, such that the system-size effect in the local order parameter is proportional to $1/(\sqrt{N_{\text{HSC}}/n_{\text{bin}}})$. If we consider $n_{\text{bin}} = 200$ histogram bins, equivalent to the number of bins used in our calculations of the density profiles, the average number of the hard spherocylinders present in each bin is $(1482/200) \sim 7$ leading to a high system-size error of ~ 0.37 in the local order parameter. One can address this problem using a rescaling procedure for $S_2(z)$ in terms of $S_{2,\infty}(z)$ the infinite system¹⁰⁸, or simply by enlarging the simulation box at the cost of increasing the computational time. We opt instead to reduce the number of

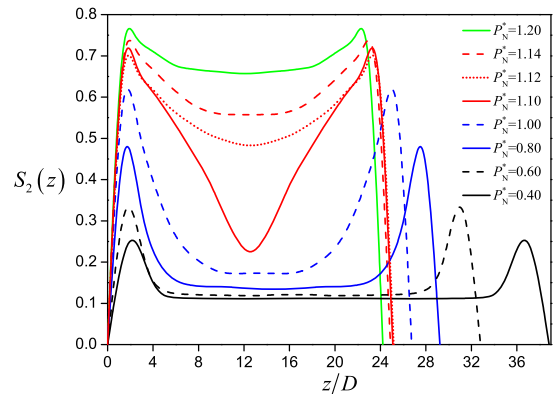


FIG. 3. Nematic order parameter profiles for a system of pure $L/D = 5$ hard spherocylinders confined between parallel hard walls obtained from $NP_N T$ -MC simulation. The curves correspond to equilibrium (normal) pressures in the range $P_N^* = [0.4 - 1.2]$ (from bottom to top).

bins to $n_{\text{bins}} = 20$, corresponding to a lower finite-size error in the calculated nematic order parameter profile of ~ 0.11 .

Throughout our work the thermodynamic variables are expressed in dimensionless units: pressure $P_N^* = P_N D^3 / (k_B T)$, number density $\rho = ND^3 / V$, and adsorption $\Gamma^* = \Gamma D^2$. All length dimensions are given in units of D .

III. RESULTS AND DISCUSSION

A. Pure hard spherocylinders in planar confinement between hard walls

We first discuss our findings for the phase behaviour of pure hard spherocylinders with an aspect ratio of $L/D = 5$ in planar confinement between parallel structureless hard walls over a wide range of equilibrium pressures (normal component of the pressure tensor) up to conditions where the bulk isotropic-nematic phase transition is found. The local density near the hard wall in the low-pressure range of $P_N^* = [0.001 - 0.1]$ is shown in Figure 2(a). At a pressure of $P_N^* \sim 0.02$ a peak in the density profile emerges at $z \sim 3D$, with the maximum of the peak becoming progressively more pronounced as the pressure is increased. The appearance of this peak is explained by the fact that for these very low density states, hard spherocylinders with an aspect ratio of $L/D = 5$ maintain their orientational freedom at $z \sim 3D$, which corresponds to half of the total length $L + D$ of the particles^{31,32}. In this low-pressure regime, the wall is actually dried (dewetted) of the rod particles. The evolution of the density profiles at higher pressures, corresponding to the range $P_N^* = [0.2 - 1.2]$, is shown in

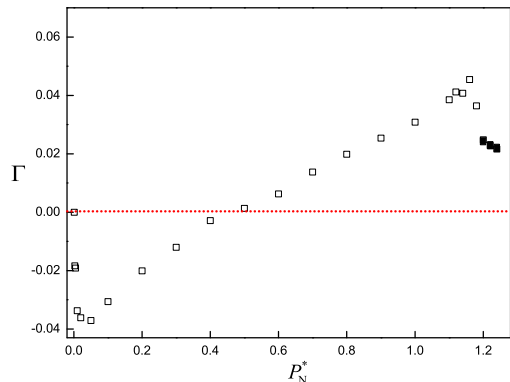


FIG. 4. Surface adsorption as a function of the equilibrium (normal) pressure P_N^* for a system of pure $L/D = 5$ hard spherocylinders confined between parallel hard walls obtained from $NP_N T$ -MC simulation. The open squares correspond to bulk isotropic states, the filled squares to bulk nematic states, and the dashed black curve is drawn to guide the eye.

317 Figure 2(b). The amplitude of the first peak at $z \sim 3D$
 318 decreases while a new peak near $z \sim D/2$ emerges and
 319 quickly becomes the dominant feature of the density profile
 320 as P_N^* is increased. The peak near $z \sim D/2$ indicates
 321 an increasing adsorption of rods at the wall correspond-
 322 ing to planar anchoring in the first wetting layer. For this
 323 pressure interval a second wetting layer is also observed
 324 between $z \sim 3D/2$ and $\sim 5D/2$, and the maximum of
 325 this peak moves closer to the wall as the pressure is in-
 326 creased indicating that the adsorbed rods are parallel to
 327 the wall. The formation of the wetting layer appears to
 328 be continuous in this case. For strongly attractive walls,
 329 one would expect the layering transition near the wall
 330 to be first-order, followed by the bulk isotropic-nematic
 331 transition.

332 In order to get deeper insight into the structure of the
 333 hard spherocylinders near the wall, the local order pa-
 334 rameter $S_2(z)$ is calculated as a function of the normal
 335 distance z (see Figure 3). We choose $S_2(z) < 0.4$ to rep-
 336 resent a disordered state and $S_2(z) > 0.4$ to represent
 337 a local nematic-like structure in similar manner as for
 338 bulk phases¹¹; though one would expect non-zero values
 339 of the nematic order parameter even for isotropic states
 340 due to finite-size effects, the choice is somewhat arbitrary.
 341 For a pressure of $P_N^* > 0.8$, the peak in $S_2(z)$ close to the
 342 wall in Figure 3 is associated with a local surface-induced
 343 nematization. As the pressure increases further, the am-
 344 plitude of the peak also increases indicating an expected
 345 enhancement of the orientational ordering of the rods at
 346 the wall.

347 We can distinguish three density (pressure) regimes for
 348 the pure component hard spherocylinders near the hard
 349 wall. In the low-density regime, corresponding to the
 350 pressure range of $P_N^* = [0.001 - 0.01]$, the density profiles
 351 increase monotonically before reaching the bulk density

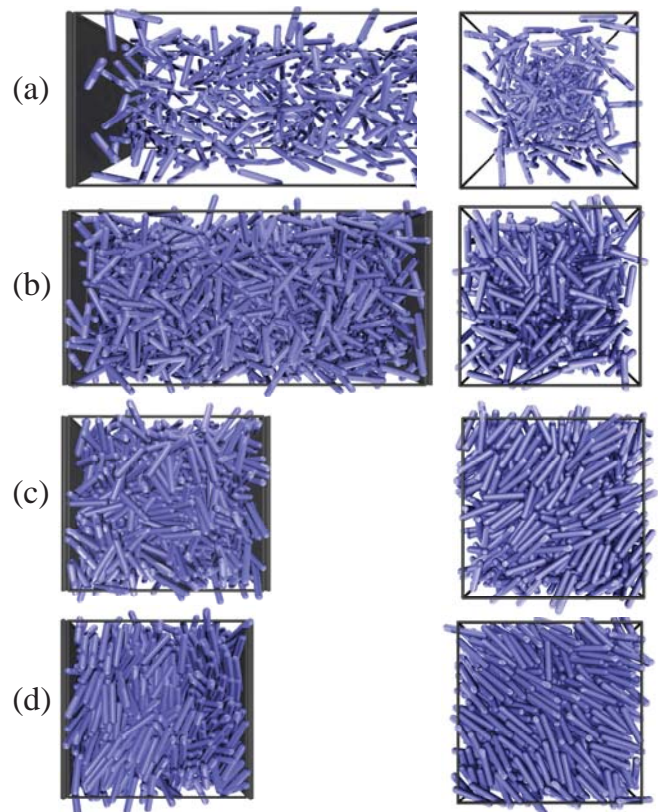


FIG. 5. Representative configurations for a system of pure $L/D = 5$ hard spherocylinders confined between parallel hard walls obtained from $NP_N T$ -MC simulation at various equilibrium (normal) pressures: (a) $P_N^* = 0.02$; (b) $P_N^* = 0.20$; (c) $P_N^* = 0.90$; and (d) $P_N^* = 1.14$. The configurations are shown in the direction parallel to the hard walls (xy plane) on the left, and in the direction perpendicular to the hard walls (along the z direction) on the right.

352 plateau. This behaviour is expected since at low densi-
 353 ties the hard rods maximize their orientational entropy
 354 when they are away from the repulsive wall. For moder-
 355 ate densities, corresponding to the pressure range of
 356 $P_N^* = [0.02 - 0.4]$, the interplay between the orientational
 357 entropy and packing effects gives rise to a non-monotonic
 358 behaviour of the density profile with a pronounced maxi-
 359 mum at $\sim (L+D)/2 = 3D$ beyond which the rods are free
 360 to rotate. The third regime seen at higher bulk densities,
 361 corresponding to the pressure range of $P_N^* = [0.6 - 1.2]$, is
 362 characterized by surface nematization with the nematic
 363 director parallel to the wall. This surface wetting is in-
 364 dicated by the shift of the first maximum in the density
 365 profile to $z \sim D/2$. The second maximum located at
 366 $z \sim 2D$ indicates an effect of the orientation of the rods
 367 (S_2 is large in this region), in contrast with what is found
 368 for the hard-sphere fluid in which case the second maxi-
 369 mum lies at $z \sim 3D/2$ ¹⁰⁹⁻¹¹¹.

370 From Figure 3 we can also observe a marked growth
 371 in the nematic order parameter in the central part of the
 372 system which occurs between $P_N^* = 1.10$ and $P_N^* = 1.14$.

373 Although we cannot exclude that the nematization of
 374 the central part can (to a minor degree) be affected by
 375 capillary effects, we associate this orientational ordering
 376 with the bulk isotropic-nematic transition of the system;
 377 the corresponding values of the bulk densities for the co-
 378 existing isotropic and nematic states are $\rho_{\text{iso}}^* = 0.0867$
 379 and $\rho_{\text{nem}}^* = 0.0941$, respectively. This result is consistent
 380 with our previously reported data⁹¹ and also with the val-
 381 ues from an earlier study¹¹ ($P^* = 1.19$, $\rho_{\text{iso}}^* = 0.0914$ and
 382 $\rho_{\text{nem}}^* = 0.0932$) obtained with isobaric-isothermal NPT -
 383 MC simulations for systems of pure hard spherocylinders
 384 with an aspect ratio of $L/D = 5$. The isotropic-nematic
 385 transition in the confined system is seen to occur at a
 386 slightly lower pressure compared to the bulk unconfined
 387 system, indicating a small degree of capillary stabiliza-
 388 tion.

389 The dependence of adsorption on the equilibrium (nor-
 390 mal) pressure is shown in Figure 4. In the low pressure
 391 regime ($P_N^* = 0.001-0.08$) the system is seen to primar-
 392 ily maximize its orientational entropy which results in
 393 the depletion of the rods particles from the vicinity of
 394 the wall. It is apparent from Figure 2(a) that for this
 395 low-pressure regime the density profiles significantly dif-
 396 fer from the corresponding bulk density limit only in the
 397 close vicinity of the wall where the local density is almost
 398 zero; it is unlikely to accommodate a randomly oriented
 399 particle in this region. The only significant contribution
 400 to the adsorption in this region is proportional to $-\rho_b L_w$
 401 where $L_w \sim (L + D)/2$ is the approximate dimension
 402 of the depleted region near the wall. The adsorption
 403 exhibits a minimum at $P_N^* \sim 0.08$ beyond which we ob-
 404 serve a near linear grow up to the IN transition. This
 405 can again be understood on the basis of our previous re-
 406 sults. In this regime, the local surface nematization oc-
 407 curs which allows for surface enhancement at the contact
 408 density $\rho(D/2)$ which is proportional to P_N according to
 409 the contact theorem. Finally, the formation of the bulk
 410 nematic phase leads to an abrupt reduction in adsorption
 411 as a result of the increment of the bulk density.

412 We conclude the analysis of pure hard spherocylinders
 413 by discussing some representative snapshots of equilib-
 414 rium configurations of selected states shown in Figure
 415 5. It can clearly be seen that at the lowest pressure
 416 ($P_N^* = 0.02$), the wall tends to be relative dry of the
 417 rod particles, while a planar anchoring is noticeable at
 418 $P_N^* = 0.20$. At even higher pressure ($P_N^* = 0.90$), the sys-
 419 tem is seen to exhibit surface nematization before experi-
 420 encing a bulk isotropic-nematic transition at $P_N^* \sim 1.14$.

421 B. Binary mixtures of hard spherocylinders and hard 422 spheres in planar confinement between hard walls

423 We are now in a position to study the influence of
 424 hard spheres on the surface behavior of binary mixtures
 425 of hard spherocylinders and hard spheres. The case of
 426 the equimolar mixture ($x_{\text{HS}} = 0.5$) is considered first.
 427 Density profiles of both species over the pressure range

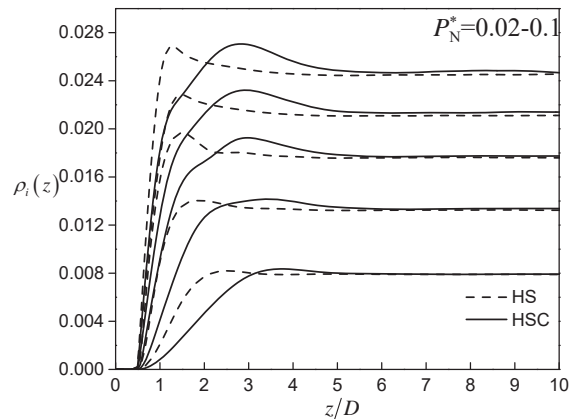


FIG. 6. Density profiles $\rho_i(z)$ of a binary equimolar mixture ($x_{\text{HS}} = 0.5$) of $L/D = 5$ hard spherocylinders (HSC, continuous curves) and hard spheres (HS, dashed curves) confined between parallel hard walls obtained from $NP_N T$ -MC simulation. The various curves correspond to states with different equilibrium (normal) pressures P_N^* : from bottom to top, $P_N^* = [0.02 - 0.1]$ with increments of $\Delta P_N^* = 0.02$.

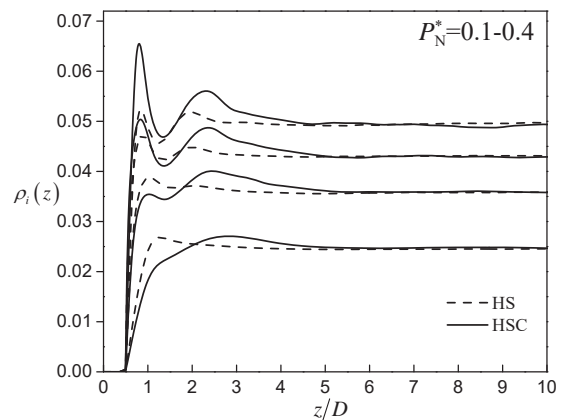


FIG. 7. Density profiles $\rho_i(z)$ of a binary equimolar mixture ($x_{\text{HS}} = 0.5$) of $L/D = 5$ hard spherocylinders (HSC, continuous curves) and hard spheres (HS, dashed curves) confined between parallel hard walls obtained from $NP_N T$ -MC simulation. The various curves correspond to states for different equilibrium (normal) pressures P_N^* : bottom to top, $P_N^* = [0.1, 0.2, 0.3, 0.4]$.

428 of $P_N^* = [0.02 - 0.1]$ are shown in Figure 6. As observed
 429 in the system of pure hard spherocylinders, these low-
 430 pressure isotropic states are characterized by a depletion
 431 of rods from the wall that maximizes their orientation
 432 entropy. In turn this creates an available volume near
 433 the wall that is free for occupation by the smaller
 434 hard-sphere particles. In view of the isotropic character

435 of the lower density states, the HSC components behave
 436 essentially like hard spheres with an effective diameter of
 437 $\sim (L + D)/2$. Consequently, the hard spheres are preferentially
 438 adsorbed at the wall and the corresponding
 439 density profiles exhibit a weak peak at $z \sim D$, while a
 440 peak in the density profiles of hard spherocylinders develops
 441 at $z \sim 3D$. The density profiles for the intermediate
 442 pressure range of $P_N^* = [0.1 - 0.4]$ is shown in Figure 7.
 443 As the pressure is increased, a new peak adjacent to the
 444 wall ($z \sim D/2$) develops in the density profile of the hard
 445 spherocylinders which exceeds the one for hard spheres
 446 for pressures $P_N^* > 0.2$ and can be attributed to the onset
 447 of the surface nematization and planar anchoring. As
 448 the pressure is further increased, the second peak in the
 449 density profile for the rods moves towards the wall from
 450 $z \sim 3D$ to $z \sim 2D$ due to propagation of the nematic
 451 ordering away from the wall; the density profiles for the
 452 hard spherocylinders is now seen to exhibit oscillations
 453 with a periodicity of D rather than $(L + D)/2$. The en-
 454 hancement of surface nematization by the rods leads to
 455 the spheres being pushed away from the wall, resulting in
 456 a reduction of the hard-sphere density near the wall re-
 457 flected by the progressively weaker amplitude of the first
 458 peak.

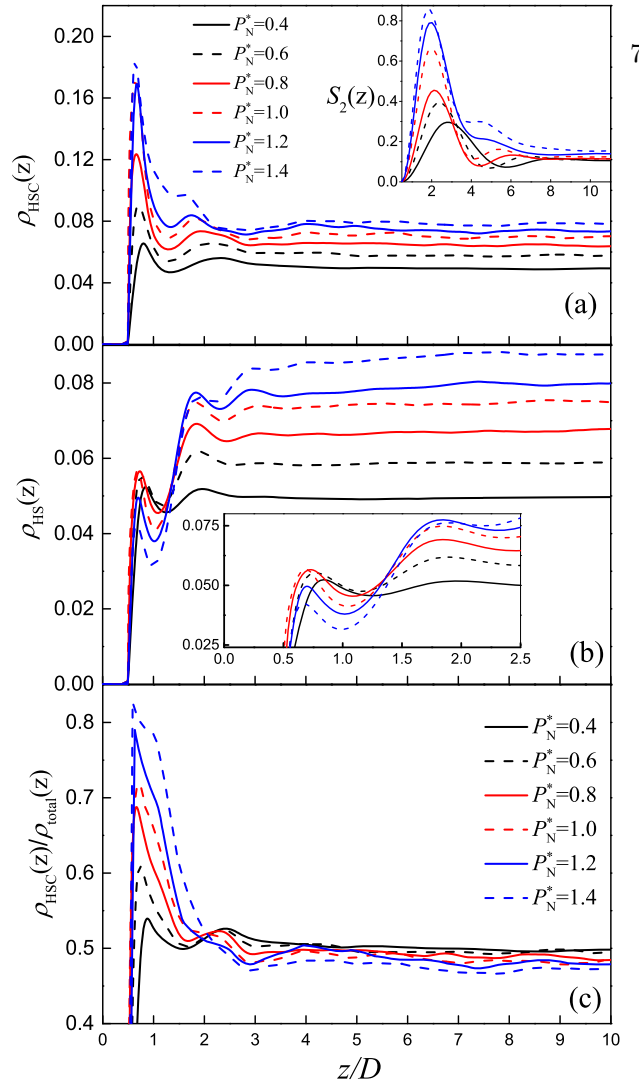


FIG. 8. Density profiles $\rho_i(z)$ for (a) $L/D = 5$ hard spherocylinders and (b) hard spheres in a binary equimolar mixture ($x_{HS} = 0.5$) confined between parallel hard walls obtained from $NP_N T$ -MC simulation. The various curves correspond to states for different equilibrium (normal) pressures P_N^* : from bottom to top, $P_N^* = [0.4 - 1.4]$. The nematic order parameter profiles $S_2(z)$ of the hard spherocylinders is shown in the inset of (a). The behaviour of the density profiles for hard spheres near a hard wall is highlighted in the inset of (b). (c) The corresponding concentration profiles $x_{HSC}(z) = \rho_{HSC}(z)/\rho_{total}(z)$.

459 The behaviour of the equimolar mixture of hard spherocylinders and hard spheres at higher equilibrium (normal) pressures in the range $P_N^* = [0.4 - 1.4]$ is shown in Figure 8. It is clear from the density profiles that higher pressures enhance the orientational ordering of the rods near the wall, which is also reflected in the behavior of the nematic order parameter seen to increase significantly near the wall. In this high-pressure regime we observe an onset of a surface nematization, although at a somewhat higher pressure ($P_N^* \sim 1.0$) than in the case of the pure hard-spherocylinder system ($P_N^* \sim 0.7$), demonstrating that the presence of hard spheres destabilizes the nematic ordering of the rods. The surface nematization leads to even stronger depletion of the hard spheres from

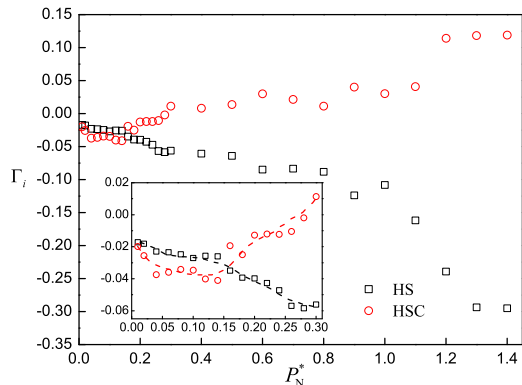


FIG. 9. Surface adsorption Γ_i ($i = \text{HSC}, \text{HS}$) of a binary equimolar mixture ($x_{\text{HS}} = 0.5$) of $L/D = 5$ hard spherocylinders (HSC, circles) and hard spheres (HS, squares) confined between parallel hard walls as a function of the equilibrium (normal) pressure P_N^* obtained from $NP_N T$ -MC simulation. The competing adsorption between the rods and spheres is highlighted in the inset. Dashed curves are drawn to guide the eye.

the wall than in the low-pressure regime, which leads to local demixing of the fluid.

The behaviour of the binary mixture can also be analysed from the surface adsorption of the hard spherocylinders (Γ_{HSC}) and hard spheres (Γ_{HS}) calculated using Eq.3 depicted in Figure 9. At low pressures, the adsorption is negative for both components, with the adsorption of hard spheres just slightly higher than that of the hard spherocylinders. However, a crossover in adsorption is observed at a pressure of $P_N^* \sim 0.16$ beyond which the rods are preferentially adsorbed. This behaviour is a consequence of the spheres being excluded from the region close to the wall due to the reorientation of the rods forming the first nematic layer. As the pressure is further increased, the preferential adsorption of hard spherocylinders becomes more evident leading eventually to a local demixing of the mixture. Representative snapshots of equilibrium configurations for equilibrium (normal) pressures ranging from the low-density isotropic states to the high-density nematic states are shown in Figure 10. The planar configuration of the rods in the high density state is clearly apparent.

It has been shown previously⁸⁸ that a presence of spherical particles in the system of rod-like particles destabilize the formation of the bulk nematic phase. Here, we analyze the impact of the presence of hard spheres on a formation of nematic films near a hard wall in binary mixtures of hard spherocylinders and hard spheres with different compositions. As shown in Figure 11 for mixtures at a fixed equilibrium (normal) pressure of $P_N^* = 1.0$ with compositions of $x_{\text{HS}} = 0, 0.1, 0.2,$ and 0.5 , thick nematic films adsorb at the wall. The thickness and the orientational order of the nematic

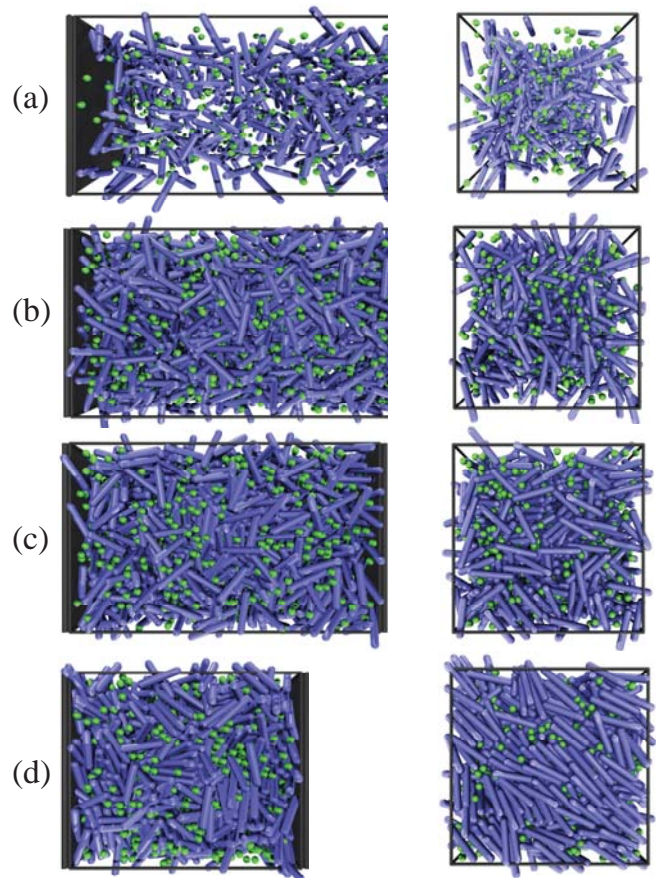


FIG. 10. Representative configurations for a binary equimolar mixture ($x_{\text{HS}} = 0.5$) of $L/D = 5$ hard spherocylinders and hard spheres confined between parallel hard walls obtained from $NP_N T$ -MC simulation at various equilibrium (normal) pressures: (a) $P_N^* = 0.04$; (b) $P_N^* = 0.26$; (c) $P_N^* = 0.60$; and (d) $P_N^* = 1.40$. The configurations are shown in the direction parallel to the hard wall (xy plane) on the left, and in the direction perpendicular to the hard wall (along the z direction) on the right.

layer is seen to decrease as the composition of spheres is decreased. We can, therefore, conclude that not only the bulk isotropic-nematic transition but also the surface nematization is destabilized by the presence of hard spheres.

Based on the previous findings one might expect the presence of high concentrations of hard spheres to weaken the preferential adsorption of rods in favour of spheres. This is, however, not the case as inferred from the dependence of the surface adsorption on the hard-sphere composition presented in Figure 12. Here, we introduce the quantity $\Delta_w = \Gamma_{\text{HSC}} - \Gamma_{\text{HS}}$ characterizing the relative adsorption of the hard spherocylinders with respect to that of the hard spheres. It is apparent that as the hard-sphere concentration is increased the adsorption of the hard spherocylinders is largely unaffected while the adsorption of the hard spheres decreases rather dramatically which is a consequence of depletion of the spheres

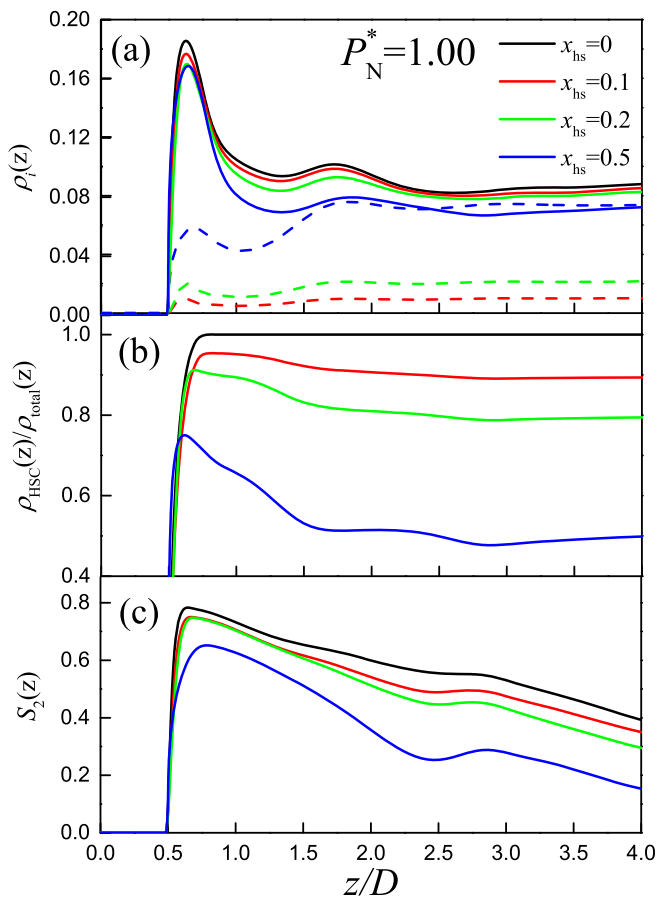


FIG. 11. (a) Density profiles $\rho_i(z)$, (b) concentration profiles $x_{\text{HSC}}(z) = \rho_{\text{HSC}}(z)/\rho_{\text{total}}(z)$, and (c) nematic order parameter profiles $S_2(z)$ for mixtures of $L/D = 5$ hard spherocylinders and hard spheres confined between parallel hard walls obtained from $NP_N T$ -MC simulation with varying overall hard-sphere composition x_{HS} at a fixed equilibrium (normal) pressure of $P_N^* = 1.0$. The continuous curves in (a) represent the density profiles of the hard spherocylinders and the dashed curves are those for the hard spheres.

524 from the wall due to surface induced nematic ordering
 525 of the rods. The extent of local demixing near the wall
 526 therefore becomes stronger as the concentration of the
 527 hard spheres in the mixture is increased. For low con-
 528 centrations of hard spheres, the effect of the presence
 529 of hard spheres is insignificant in terms of adsorption of
 530 hard spherocylinders in the nematic layer since the hard
 531 spheres are depleted from the wall in the high-pressure
 532 regime. It is only when $x_{hs} \sim 0.5$ that the presence of
 533 hard spheres can influence the order parameter apprecia-
 534 bly.

535 IV. CONCLUSIONS

536 We have studied structure, orientational ordering and
 537 phase behaviour of pure hard spherocylinders and of bi-
 538 nary mixtures of hard spherocylinders and hard spheres

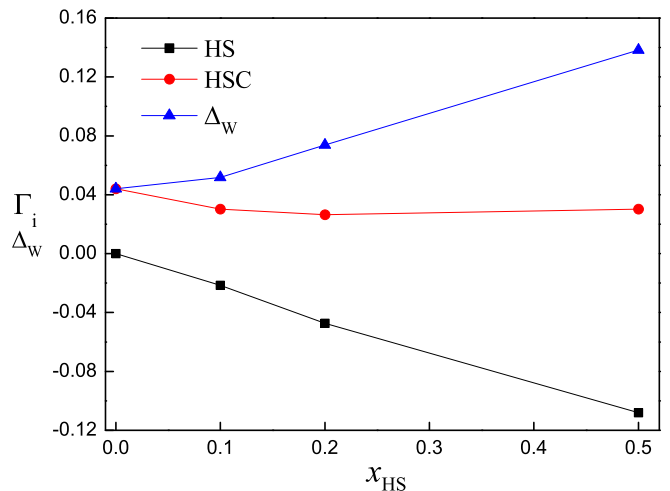


FIG. 12. Dependence of surface adsorption on the overall hard-sphere composition x_{HS} for mixtures of $L/D = 5$ hard spherocylinders and hard spheres confined between parallel hard walls obtained from $NP_N T$ -MC simulation at a fixed equilibrium (normal) pressure of $P_N^* = 1.0$. The trend for the differential adsorption $\Delta_w = \Gamma_{\text{HSC}} - \Gamma_{\text{HSC}}$ is also included.

539 confined between parallel hard walls using constant nor-
 540 mal pressure MC simulations. The aspect ratio of the
 541 hard spherocylinders considered is $L/D = 5$ and the
 542 hard-sphere diameter is taken to be the same as the cylin-
 543 der diameter D . States up to the bulk isotropic-nematic
 544 transition are examined.

545 Starting with surface properties of pure rods, we find
 546 that at low-pressure (low-density) states the system is
 547 fully isotropic resulting in a depletion of the particles
 548 from the hard wall in order to maximize the (dominant)
 549 contribution to the orientational entropy. At higher pres-
 550 sures, packing effects prevail and the rods adsorb at the
 551 wall with a near-linear dependence of the adsorption with
 552 pressure. This process is accompanied by a surface nematic-
 553 ization with the nematic director oriented parallel to the
 554 wall and the induced nematic film growing continuously
 555 up to the bulk isotropic-nematic transition.

556 The main objective of our study is a detailed exam-
 557 ination of the effect of the surface on the properties of
 558 binary mixtures of rod-like and spherical particles. Here,
 559 the competition between the orientational entropy and
 560 packing effects near the wall leads to a local demixing of
 561 the mixture. At low pressures (densities) we observe a
 562 preferential adsorption of hard spheres that fill the free
 563 volume left by the rods near the wall from which the
 564 rods are depleted due to orientational entropy effects.
 565 This effect is, however, quite mild. At higher pressures,
 566 a crossover in the preferential surface adsorption occurs
 567 beyond which the local demixing near the wall is seen to
 568 increase with the pressure. In this regime, the rod parti-
 569 cles adsorb at the wall to form a nematic film the width
 570 of which increases continuously as the isotropic-nematic
 571 transition is approached. The process is accompanied by
 572 an increase in the nematic order parameter and deple-

tion of the hard-sphere particles from the wall which in turn leads to local demixing. This process is continuous as we only consider states (pressures) corresponding to bulk isotropic phases. Sudden changes in the structure of the fluid are expected for even higher pressures which exceed the isotropic-nematic transition, as is observed in Figure 4 for the pure component hard-spherocylinder system. Overall, however, one can conclude that the presence of hard spheres is found to destabilize the surface nematization, and an increase in the hard-sphere concentration enhances demixing.

In our current work we focus exclusively on isotropic and nematic states. Smectic order of rod particles in confinement²⁸ and layering in rod-sphere mixtures¹¹² are examples of other surface induced structures occurring at higher pressures. A feature which has been omitted in our study is an analysis of the expected biaxiality and of the rod-like particles close to wall and the fluid-wall interfacial tension^{33,57,58}. The method adopted in our current study to characterize the spatial distribution of the order parameter tensor is not sufficiently accurate to compute the biaxiality of HSCs induced by the surface. We postpone this to future work, and we also plan to use advanced DFT methodologies^{12,85,113} to predict the surface behaviour of mixtures of rods and spheres including a detailed comparison with simulation.

ACKNOWLEDGMENTS

LW thanks the Department for Business Innovation and Skills of the UK and China Scholarship Council for funding a PhD studentship. The MC simulations were performed using the High Performance Computing service provided by Imperial College London. AM acknowledges support from the Czech Science Foundation, project 16-12291S. Funding to the Molecular Systems Engineering Group from the Engineering and Physical Sciences Research Council (EPSRC) of the UK (grants GR/T17595, GR/N35991, EP/E016340, and EP/J014958), the Joint Research Equipment Initiative (JREI) (GR/M94426), and the Royal Society-Wolfson Foundation refurbishment scheme is also gratefully acknowledged.

¹F. A. Escobedo, "Engineering entropy in soft matter: the bad, the ugly and the good," *Soft Matter* **10**, 8388–8400 (2014).

²V. N. Manoharan, "Colloidal matter: Packing, geometry, and entropy," *Science* **349**, 1253751 (2015).

³S. C. Glotzer and M. J. Solomon, "Anisotropy of building blocks and their assembly into complex structures," *Nat. Mater.* **6**, 557–562 (2007).

⁴P. F. Damasceno, M. Engel, and S. C. Glotzer, "Predictive self-assembly of polyhedra into complex structures," *Science* **337**, 453–457 (2012).

⁵G. van Anders, N. K. Ahmed, R. Smith, M. Engel, and S. C. Glotzer, "Entropically patchy particles: engineering valence through shape entropy," *ACS Nano* **8**, 931–940 (2014).

⁶C. Avendaño, G. Jackson, E. A. Müller, and F. A. Escobedo, "Assembly of porous smectic structures formed

from interlocking high-symmetry planar nanorings," *Proc. Nat. Acad. Sci.* **113**, 9699–9703 (2016).

⁷C. Avendaño and F. A. Escobedo, "Packing, entropic patchiness, and self-assembly of non-convex colloidal particles: a simulation perspective," *Curr. Opin. Colloid Interface Sci.* **30**, 62–69 (2017).

⁸A. Yethiraj and A. van Blaaderen, "A colloidal model system with an interaction tunable from hard sphere to soft and dipolar," *Nature* **421**, 513–517 (2003).

⁹L. Onsager, "The effects of shape on the interaction of colloidal particles," *Ann. N. Y. Acad. Sci.* **51**, 627–659 (1949).

¹⁰D. Frenkel, "Onsager's spherocylinders revisited," *J. Phys. Chem.* **91**, 4912–4916 (1987).

¹¹S. C. McGrother, D. C. Williamson, and G. Jackson, "A re-examination of the phase diagram of hard spherocylinders," *J. Chem. Phys.* **104**, 6755–6771 (1996).

¹²H. Hansen-Goos and K. Mecke, "Fundamental measure theory for inhomogeneous fluids of nonspherical hard particles," *Phys. Rev. Lett.* **102**, 018302 (2009).

¹³P. G. Bolhuis and D. Frenkel, "Tracing the phase boundaries of hard spherocylinders," *J. Chem. Phys.* **106**, 666–687 (1997).

¹⁴H. Löwen, "Colloidal dispersions in external fields: recent developments," *J. Phys. Condes. Matter* **20**, 404201 (2008).

¹⁵R. Evans, U. M. B. Marconi, and P. Tarazona, "Fluids in narrow pores: Adsorption, capillary condensation, and critical points," *J. Chem. Phys.* **84**, 2376 (1986).

¹⁶B. Jérôme, "Surface effects and anchoring in liquid crystals," *Rep. Prog. Phys.* **54**, 391–451 (1991).

¹⁷T. J. Sluckin, "Anchoring transitions at liquid crystal surfaces," *Phys. A* **213**, 105–109 (1995).

¹⁸P. Sheng, "Phase transition in surface-aligned nematic films," *Phys. Rev. Lett.* **37**, 1059–1062 (1976).

¹⁹M. M. Telo da Gama, "The interfacial properties of a model of a nematic liquid-crystal .1. the nematic-isotropic and the nematic-vapor interfaces," *Mol. Phys.* **52**, 585–610 (1984).

²⁰M. M. Telo da Gama, "The interfacial properties of a model of a nematic liquid-crystal .2. induced orientational order and wetting transitions at a solid fluid interface," *Mol. Phys.* **52**, 611–630 (1984).

²¹M. M. Telo da Gama, P. Tarazona, M. P. Allen, and R. Evans, "The effect of confinement on the isotropic nematic transition," *Mol. Phys.* **71**, 801–821 (1990).

²²A. Poniewierski and T. J. Sluckin, "Statistical-mechanics of a simple-model of the nematic liquid crystal-wall interface," *Mol. Cryst. Liq. Cryst.* **111**, 373–386 (1984).

²³A. Poniewierski and T. J. Sluckin, "Theory of the nematic-isotropic transition in a restricted geometry," *Liq. Cryst.* **2**, 281–311 (1987).

²⁴A. Poniewierski and R. Holyst, "Nematic alignment at a solid substrate: The model of hard spherocylinders near a hard wall," *Phys. Rev. A* **38**, 3721–3727 (1988).

²⁵A. Poniewierski, "Ordering of hard needles at a hard wall," *Physical Review E* **47**, 3396 (1993).

²⁶R. van Roij, M. Dijkstra, and R. Evans, "Interfaces, wetting, and capillary nematization of a hard-rod fluid: Theory for zwanzig model," *J. Chem. Phys.* **113**, 7689–7701 (2000).

²⁷R. Aliabadi, M. Moradi, and S. Varga, "Orientational ordering of confined hard rods: The effect of shape anisotropy on surface ordering and capillary nematization," *Phys. Rev. E* **92**, 032503 (2015).

²⁸A. Maliješvský and S. Varga, "Phase behaviour of parallel hard rods in confinement: an onsager theory study," *J. Phys. Condes. Matter* **22**, 175002 (2010).

²⁹S. Ye, P. Zhang, and J. Z. Y. Chen, "Surface-induced phase transitions of wormlike chains in slit confinement," *Soft Matter* **12**, 2948–2959 (2016).

³⁰L. Qin and J. Z. Y. Chen, "Recent theoretical development in confined liquid-crystal polymers," *Acta Phys. Sin.* **65**, 174201 (2016).

³¹Y. Mao, M. E. Cates, and H. N. W. Lekkerkerker,

- 699 “Theory of the depletion force due to rodlike polymer,”
700 *J. Chem. Phys.* **106**, 3721–3729 (1997).
- 701 ³²Y. Mao, P. Bladon, H. N. W. Lekkerkerker, and M. E. Cates,
702 “Density profiles and thermodynamics of rod-like particles be-
703 tween parallel walls,” *Mol. Phys.* **92**, 151–159 (1997).
- 704 ³³M. Dijkstra, R. van Roij, and R. Evans, “Wetting and cap-
705 illary nematization of a hard-rod fluid: A simulation study,”
706 *Phys. Rev. E.* **63**, 051703 (2001).
- 707 ³⁴D. de las Heras, E. Velasco, and L. Mederos, “Effects of wet-
708 ting and anchoring on capillary phenomena in a confined liquid
709 crystal,” *J. Chem. Phys.* **120**, 4949–4957 (2004).
- 710 ³⁵M. Dijkstra and R. van Roij, “Entropic wetting in colloidal par-
711 ticles,” *J. Phys. Condens. Matter* **17**, S3507–S3514 (2005).
- 712 ³⁶S. Jungblut, R. Tuinier, K. Binder, and T. Schilling, “Depletion
713 induced isotropic-isotropic phase separation in suspensions of
714 rod-like colloids,” *J. Chem. Phys.* **127**, 244909 (2007).
- 715 ³⁷M. Allen, “Molecular simulation and theory of liquid crystal
716 surface anchoring,” *Mol. Phys.* **96**, 1391–1397 (1999).
- 717 ³⁸M. P. Allen, “Molecular simulation and theory of the isotropic-
718 nematic interface,” *J. Chem. Phys.* **112**, 5547–5453 (2000).
- 719 ³⁹M. M. Pineiro, A. Galindo, and A. O. Parry, “Surface ordering
720 and capillary phenomena of confined hard cut-sphere particles,”
721 *Soft Matter* **3**, 768–778 (2007).
- 722 ⁴⁰C. Avendano, C. M. Liddell Watson, and F. A. Escobedo,
723 “Directed self-assembly of spherical caps via confinement,”
724 *Soft Matter* **9**, 9153–9166 (2013).
- 725 ⁴¹K. Muangnapoh, C. Avendano, F. A. Escobedo, and C. M. Lid-
726 dell Watson, “Degenerate crystals from colloidal dimers under
727 confinement,” *Soft Matter* **10**, 9729–9738 (2014).
- 728 ⁴²F. Barmes and D. J. Cleaver, “Computer simulation of a liquid-
729 crystal anchoring transition,” *Phys. Rev. E.* **69**, 061705 (2004).
- 730 ⁴³T. Gruhn and M. Schoen, “Substrate-induced order
731 in confined nematic liquid-crystal films,”
732 *J. Chem. Phys.* **108**, 9124–9136 (1998).
- 733 ⁴⁴E. A. Müller, I. Rodríguez-Ponce, A. Oualid, J. M. Romero-
734 Enrique, and L. F. Rull, “Wetting of planar surfaces by a gay-
735 berne liquid crystal,” *Mol. Sim.* **29**, 385–391 (2003).
- 736 ⁴⁵L. F. Rull, J. M. Romero-Enrique, and E. A. Müller,
737 “Observation of surface nematization at the solid-
738 liquid crystal interface via molecular simulation,”
739 *J. Phy. Chem. C* **111**, 15998–16005 (2007).
- 740 ⁴⁶Q. Ji, R. Lefort, and D. Morineau, “Influence of pore shape
741 on the structure of a nanoconfined gay-berne liquid crystal,”
742 *Chem. Phys. Lett.* **478**, 161–165 (2009).
- 743 ⁴⁷M. Greschek and M. Schoen, “Orientational prewetting
744 of planar solid substrates by a model liquid crystal,”
745 *J. Chem. Phys.* **135**, 204702 (2011).
- 746 ⁴⁸V. A. Ivanov, A. S. Rodionova, J. A. Martemyanova, M. R.
747 Stukan, M. Müller, W. Paul, and K. Binder, “Wall-induced
748 orientational order in athermal semidilute solutions of semi-
749 flexible polymers: Monte carlo simulations of a lattice model,”
750 *J. Chem. Phys.* **138**, 234903 (2013).
- 751 ⁴⁹V. A. Ivanov, A. S. Rodionova, J. A. Martemyanova, M. R.
752 Stukan, M. Müller, W. Paul, and K. Binder, “Confor-
753 mational properties of semiflexible chains at nematic order-
754 ing transitions in thin films: A monte carlo simulation,”
755 *Macromolecules* **47**, 1206–1220 (2014).
- 756 ⁵⁰A. Milchev, S. A. Egorov, and K. Binder, “Semiflexible
757 polymers confined in a slit pore with attractive walls: two-
758 dimensional liquid crystalline order versus capillary nematiza-
759 tion,” *Soft Matter* **13**, 1888–1903 (2017).
- 760 ⁵¹S. A. Egorov, A. Milchev, and K. Binder,
761 “Capillary nematization of semiflexible polymers,”
762 *Macromol. Theory Simul.* **26**, 1600036 (2017).
- 763 ⁵²S. Varga and G. Jackson, “Simulation of the macroscopic
764 pitch of a chiral nematic phase of a model chiral mesogen,”
765 *Chem. Phys. Lett.* **377**, 6–12 (2003).
- 766 ⁵³S. Varga and G. Jackson, “Study of the pitch of fluids of elec-
767 trostatically chiral anisotropic molecules: mean-field theory and
768 simulation,” *Mol. Phys.* **104**, 3681–3691 (2006).
- 769 ⁵⁴D. L. Cheung and F. Schmid, “Monte carlo sim-
770 ulations of liquid crystals near rough walls,”
771 *Journal of Chemical Physics* **122**, 074902 (2005).
- 772 ⁵⁵H. Steuer, S. Hess, and M. Schoen, “Phase be-
773 havior of liquid crystals confined by smooth walls,”
774 *Phys. Rev. E.* **69**, 031708 (2004).
- 775 ⁵⁶Y. Trukhina and T. Schilling, “Computer simulation
776 study of a liquid crystal confined to a spherical cavity,”
777 *Phys. Rev. E.* **77**, 011701 (2008).
- 778 ⁵⁷P. E. Brumby, A. J. Haslam, E. de Miguel, and G. Jackson,
779 “Subtleties in the calculation of the pressure and pressure ten-
780 sor of anisotropic particles from volume-perturbation methods
781 and the apparent asymmetry of the compressive and expansive
782 contributions,” *Mol. Phys.* **109**, 169–189 (2011).
- 783 ⁵⁸P. E. Brumby, H. H. Wensink, A. J. Haslam, and G. Jackson,
784 “Structure and interfacial tension of a hard-rod fluid in planar
785 confinement,” *Langmuir* **33**, 11754–11770 (2017).
- 786 ⁵⁹S. V. Savenko and M. Dijkstra, “Sedimentation and mul-
787 tiphase equilibria in suspensions of colloidal hard rods,”
788 *Phys. Rev. E.* **70**, 051401 (2004).
- 789 ⁶⁰H. Zocher, *Z. Anorg. Chem.* **147**, 91 (1925).
- 790 ⁶¹F. M. van der Kooij, K. Kassapidou, and H. N. W. Lekkerker-
791 kerker, “Liquid crystal phase transitions in suspensions of poly-
792 disperse plate-like particles,” *Nature* **406**, 868 (2000).
- 793 ⁶²H. H. Wensink and H. N. W. Lekkerkerker, “Phase di-
794 agram of hard colloidal platelets: a theoretical account,”
795 *Molecular Physics* **107**, 2111–2118 (2009).
- 796 ⁶³M. Bravo-Sanchez, T. J. Simmons, and M. A. Vidal,
797 “Liquid crystal behavior of single wall carbon nanotubes,”
798 *Carbon* **48**, 3531–3542 (2010).
- 799 ⁶⁴R. Mezzenga, J.-M. Jung, and J. Adamcik, “Effects
800 of charge double layer and colloidal aggregation on the
801 isotropic-nematic transition of protein fibers in water,”
802 *Langmuir* **26**, 10401–10405 (2010).
- 803 ⁶⁵V. A. Parsegian and S. L. Brenner, “The role of long
804 range forces in ordered arrays of tobacco mosaic virus,”
805 *Nature* **259**, 632–635 (1976).
- 806 ⁶⁶Z. Dogic and S. Fraden, “Smectic phase in a col-
807 loidal suspension of semiflexible virus particles,”
808 *Phys. Rev. Lett.* **78**, 2417–2420 (1997).
- 809 ⁶⁷K. R. Purdy, S. Varga, A. Galindo, G. Jackson, and S. Fraden,
810 “Nematic phase transitions in mixtures of thin and thick col-
811 loidal rods,” *Phys. Rev. Lett.* **94**, 057801 (2005).
- 812 ⁶⁸W. G. Miller, C. C. Wu, E. L. Wee, G. L. San-
813 tee, J. H. Rai, and K. G. Goebel, “Thermody-
814 namics and dynamics of polypeptide liquid crystals,”
815 *Pure and Applied Chemistry* **38**, 37–58 (1974).
- 816 ⁶⁹J. C. Horton, A. M. Donald, and A. Hill, “Coexistence of two
817 liquid crystalline phases in poly(benzyl-l-glutamate) solutions,”
818 *Nature* **346**, 44–45 (1990).
- 819 ⁷⁰M. Nakata, G. Zanchetta, B. D. Chapman, C. D. Jones, J. O.
820 Cross, R. Pindak, T. Bellini, and N. A. Clark, “End-to-end
821 stacking and liquid crystal condensation of 6- to 20-base pair
822 dna duplexes,” *Science* **318**, 1276–1279 (2007).
- 823 ⁷¹J. Galanis, D. Harries, D. L. Sackett, W. Losert, and
824 R. Nossal, “Spontaneous patterning of confined granular rods,”
825 *Phys. Rev. Lett.* **96**, 028002 (2006).
- 826 ⁷²A. Kuijk, D. V. Byelov, A. V. Petukhov, A. van Blaaderen,
827 and A. Imhof, “Phase behavior of colloidal silica rods,”
828 *Farad. Discuss.* **159**, 181–199 (2012).
- 829 ⁷³A. Stroobants, H. N. W. Lekkerkerker, and D. Frenkel, “Evi-
830 dence for smectic order in a fluid of hard parallel spherocylin-
831 ders,” *Phys. Rev. Lett.* **57**, 1452–1455 (1986).
- 832 ⁷⁴D. Frenkel, H. N. W. Lekkerkerker, and A. Stroobants, “Ther-
833 modynamic stability of a smectic phase in a system of hard
834 rods,” *Nature* **332**, 822–823 (1988).
- 835 ⁷⁵J. A. C. Veerman and D. Frenkel, “Phase diagram of a
836 system of hard spherocylinders by computer simulation,”
837 *Phys. Rev. A* **41**, 3237–3244 (1990).
- 838 ⁷⁶M. P. Allen, G. T. Evans, D. Frenkel, and B. M. Mulder, “Hard

- convex body fluids," *Adv. Chem. Phys.* **86**, 1–166 (1993).
- ⁷⁷H. N. W. Lekkerkerker, P. Coulon, R. V. D. Haegen, and R. Deblieck, "On the isotropic liquid crystal phase separation in a solution of rodlike particles of different lengths," *J. Chem. Phys.* **80**, 3427–3433 (1984).
- ⁷⁸T. Odijk and H. N. W. Lekkerkerker, "Theory of the isotropic-liquid crystal phase separation for a solution of bidisperse rodlike macromolecules," *J. Phys. Chem.* **89**, 2090–2096 (1985).
- ⁷⁹R. van Roij and B. Mulder, "Absence of high-density consolute point in nematic hard rod mixtures," *J. Chem. Phys.* **105**, 11237–11245 (1996).
- ⁸⁰S. Varga, K. Purdy, A. Galindo, S. Fraden, and G. Jackson, "Nematic-nematic phase separation in binary mixtures of thick and thin hard rods: Results from Onsager-like theories," *Phys. Rev. E* **72**, 051704 (2005).
- ⁸¹P. G. Bolhuis and D. Frenkel, "Numerical study of the phase diagram of a mixture of spherical and rodlike colloids," *J. Chem. Phys.* **101**, 9869–9875 (1994).
- ⁸²G. A. Vliegenthart and H. N. W. Lekkerkerker, "Phase behavior of colloidal rod-sphere mixtures," *J. Chem. Phys.* **111**, 4153–4157 (1999).
- ⁸³G. H. Koenderink, G. A. Vliegenthart, S. G. J. M. Kluijtmans, A. van Blaaderen, A. P. Philipse, and H. N. W. Lekkerkerker, "Depletion-induced crystallization in colloidal rod-sphere mixtures," *Langmuir* **15**, 4693–4696 (1999).
- ⁸⁴M. Schmidt, "Density functional theory for colloidal rod-sphere mixtures," *Phys. Rev. E* **63**, 050201 (2001).
- ⁸⁵R. Roth, J. M. Brader, and M. Schmidt, "Entropic wetting of a colloidal rod-sphere mixture," *Europhys. Letter* **63**, 549–555 (2003).
- ⁸⁶M. Schmidt and J. M. Brader, "Hard sphere fluids in random fiber networks," *J. Chem. Phys.* **119**, 3495–3500 (2003).
- ⁸⁷N. Urakami and M. Imai, "Dependence on sphere size of the phase behavior of mixtures of rods and spheres," *J. Chem. Phys.* **119**, 2463–2470 (2003).
- ⁸⁸S. Lago, A. Cuetos, B. Martínez-Haya, and L. F. Rull, "Crowding effects in binary mixtures of rod-like and spherical particles," *J. Mol. Recogn.* **17**, 417–425 (2004).
- ⁸⁹A. Cuetos, B. Martínez-Haya, S. Lago, and L. F. Rull, "Use of parsons-lee and onsager theories to predict nematic and demixing behavior in binary mixtures of hard rods and hard spheres," *Phys. Rev. E* **75**, 061701 (2007).
- ⁹⁰G. Cinacchi and L. D. Gaetani, "Diffusion in the lamellar phase of a rod-sphere mixture," *J. Chem. Phys.* **131**, 104908 (2009).
- ⁹¹L. Wu, A. Malijevský, G. Jackson, E. A. Müller, and C. Avendaño, "Orientational ordering and phase behaviour of binary mixtures of hard spheres and hard spherocylinders," *J. Chem. Phys.* **143**, 044906 (2015).
- ⁹²A. Stroobants and H. N. W. Lekkerkerker, "Liquid crystal phase transitions in a solution of rodlike and disklike particles," *J. Phys. Chem.* **88**, 3669–3674 (1984).
- ⁹³A. G. Vanakaras, S. C. McGrother, G. Jackson, and D. J. Photinos, "Hydrogen-bonding and phase biaxiality in nematic rod-plate mixtures," *Mol. Cryst. Liq. Cryst.* **323**, 199–209 (1998).
- ⁹⁴F. M. van der Kooij and H. N. W. Lekkerkerker, "Liquid-crystalline phase behavior of a colloidal rod-plate mixture," *Phys. Rev. Lett.* **84**, 781–784 (2000).
- ⁹⁵A. Galindo, G. Jackson, and D. J. Photinos, "Computer simulation of the interface between two liquid crystalline phases in rod-plate binary mixtures," *Chem. Phys. Lett.* **325**, 631–638 (2000).
- ⁹⁶H. H. Wensink, G. J. Vroege, and H. N. W. Lekkerkerker, "Biaxial versus uniaxial nematic stability in asymmetric rod-plate mixtures," *Phys. Rev. E* **66**, 041704 (2002).
- ⁹⁷S. Varga, A. Galindo, and G. Jackson, "Ordering transitions, biaxiality, and demixing in the symmetric binary mixture of rod and plate molecules described with the onsager theory," *Phys. Rev. E* **66**, 011707 (2002).
- ⁹⁸A. Galindo, A. J. Haslam, S. Varga, G. Jackson, A. G. Vanakaras, D. J. Photinos, and D. A. Dunmur, "The phase behavior of a binary mixture of rodlike and dislike mesogens: Monte carlo simulation, theory, and experiment," *J. Chem. Phys.* **119**, 5216–5225 (2003).
- ⁹⁹A. Cuetos, A. Galindo, and G. Jackson, "Thermotropic biaxial liquid crystalline phases in a mixture of attractive uniaxial rod and disk particles," *Phys. Rev. Lett.* **101**, 237802 (2008).
- ¹⁰⁰H. H. Wensink, G. J. Vroege, and H. N. W. Lekkerkerker, "Isotropic-nematic density inversion in a binary mixture of thin and thick hard platelets," *J Phys. Chem. B* **105**, 10610–10618 (2001).
- ¹⁰¹A. A. Verhoeff, H. H. Wensink, M. Vis, G. Jackson, and H. N. W. Lekkerkerker, "Liquid crystal phase transitions in systems of colloidal platelets with bimodal shape distribution," *J Phys. Chem. B* **113**, 13476–13484 (2009).
- ¹⁰²F. Gámez, R. D. Acemel, and A. Cuetos, "Demixing and nematic behaviour of oblate hard spherocylinders and hard spheres mixtures: Monte carlo simulation and parsons-lee theory," *Mol. Phys.* **111**, 3136 (2013).
- ¹⁰³A. Malijevský, G. Jackson, and S. Varga, "Many-fluid onsager density functional theories for orientational ordering in mixtures of anisotropic hard-body fluids," *J. Chem. Phys.* **129**, 144504 (2008).
- ¹⁰⁴J. M. Brader, A. Esztermann, and M. Schmidt, "Colloidal rod-sphere mixtures: Fluid-fluid interfaces and the onsager limit," *Phys. Rev. E* **66**, 031401 (2002).
- ¹⁰⁵P. G. de Gennes and J. Prost, *The Physics of Liquid Crystals*, 2nd ed. (Oxford University Press, Oxford, 1993).
- ¹⁰⁶W. H. Press, S. A. Teukolsky, and W. T. e. a. Vetterling, *Numerical Recipes in FORTRAN: the art of scientific computing*, 2nd ed. (Cambridge University Press, Cambridge, 1992).
- ¹⁰⁷R. Eppenga and D. Frenkel, "Monte-carlo study of the isotropic and nematic phases of infinitely thin hard platelets," *Mol. Phys* **52**, 1303–1334 (1984).
- ¹⁰⁸A. Richter and T. Gruhn, "Structure formation and fractionation in systems of polydisperse attractive rods," *J. Chem. Phys.* **125**, 064908 (2006).
- ¹⁰⁹J. R. Henderson and F. Van Swol, "On the interface between a fluid and a planar wall - theory and simulations of a hard-sphere fluid at a hard-wall," *Mol. Phys* **51**, 991–1010 (1984).
- ¹¹⁰J. R. Henderson and F. van Swol, "Grand potential densities of wallliquid interfaces approaching complete drying," *J. Chem. Phys.* **89**, 5010–5014 (1988).
- ¹¹¹F. van Swol and J. R. Henderson, "Wetting and drying transitions at a fluid-wall interface: Density-functional theory versus computer simulation," *Phys. Rev. A* **40**, 2567–2578 (1989).
- ¹¹²M. Adams, Z. Dogic, S. Keller, and S. Fraden, "Entropically driven microphase transitions in mixtures of colloidal rods and spheres," *Nature* **393**, 349–352 (1998).
- ¹¹³H. Hansen-Goos and K. Mecke, "Tensorial density functional theory for non-spherical hard-body fluids," *J. Phys. Condens. Matter* **22**, 364107 (2010).